The Plant Cell, Vol. 19: 2531–2543, August 2007, www.plantcell.org

Arabidopsis TRANSPARENT TESTA GLABRA2 Is Directly Regulated by R2R3 MYB Transcription Factors and Is Involved in Regulation of *GLABRA2* Transcription in Epidermal Differentiation [W]

Tetsuya Ishida,[a] Sayoko Hattori,[a] Ryosuke Sano,[a,1] Kayoko Inoue,[a,2] Yumiko Shirano,[b,3] Hiroaki Hayashi,[c,4] Daisuke Shibata,[b,1] Shusei Sato,[d] Tomohiko Kato,[d,5] Satoshi Tabata,[d] Kiyotaka Okada,[a,e,6] and Takuji Wada[a,7]

[a] Plant Science Center, RIKEN, Tsurumi-ku, Yokohama, Kanagawa 230-0045, Japan
[b] Mitsui Plant Biotechnology Research Institute, Tsukuba, Ibaraki 305-0047, Japan
[c] Department of Applied Biological Chemistry, Graduate School of Agricultural and Life Sciences, University of Tokyo, Bunkyo-ku, Tokyo 113-8657, Japan
[d] Kazusa DNA Research Institute, Kisarazu, Chiba 292-0818, Japan
[e] Department of Botany, Graduate School of Science, Kyoto University, Sakyo-ku, Kyoto 606-8502, Japan

***Arabidopsis thaliana TRANSPARENT TESTA GLABRA2* (*TTG2*) encodes a WRKY transcription factor and is expressed in young leaves, trichomes, seed coats, and root hairless cells. An examination of several trichome and root hair mutants indicates that *MYB* and *bHLH* genes regulate *TTG2* expression. Two MYB binding sites in the *TTG2* 5′ regulatory region act as *cis* regulatory elements and as direct targets of R2R3 MYB transcription factors such as WEREWOLF, GLABRA1, and TRANSPARENT TESTA2. Mutations in *TTG2* cause phenotypic defects in trichome development and seed color pigmentation. Transgenic plants expressing a chimeric repressor version of the TTG2 protein (TTG2:SRDX) showed defects in trichome formation, anthocyanin accumulation, seed color pigmentation, and differentiation of root hairless cells. *GLABRA2* (*GL2*) expression was markedly reduced in roots of *ProTTG2:TTG2:SRDX* transgenic plants, suggesting that *TTG2* is involved in the regulation of *GL2* expression, although *GL2* expression in the *ttg2* mutant was similar to that in the wild type. Our analysis suggests a new step in a regulatory cascade of epidermal differentiation, in which complexes containing R2R3 MYB and bHLH transcription factors regulate the expression of *TTG2*, which then regulates *GL2* expression with complexes containing R2R3 MYB and bHLH in the differentiation of trichomes and root hairless cells.**

INTRODUCTION

Cell differentiation and morphogenesis at the appropriate time and place are critical for the normal development of multicellular organisms. In plants, root hairs and trichomes are differentiated from epidermal cells of the root and the shoot, respectively. Molecular genetic analyses have been pursued in *Arabidopsis thaliana* to understand the regulation of cellular differentiation programs and have revealed a network of transcriptional regulators that control the development of these organs.

In *Arabidopsis*, root epidermal cells differentiate into either root hair cells or hairless cells in a position-dependant manner. Epidermal cells that are in contact with two underlying cortical cells (H cells) differentiate into root hair cells, whereas epidermal cells in contact with a single cortical cell (N cells) usually do not generate root hairs and become hairless cells as their final developmental form (Dolan et al., 1994). Several genes involved in controlling root hair patterning have been identified. *WEREWOLF* (*WER*) encodes an R2R3 MYB transcription factor, *TRANSPARENT TESTA GLABRA1* (*TTG1*) encodes a WD40 protein, and *GLABRA2* (*GL2*) encodes a homeodomain–leucine zipper (HD-ZIP) transcription factor, all of which are required to specify hairless cells (Galway et al., 1994; Rerie et al., 1994; Di Cristina et al., 1996; Masucci et al., 1996; Lee and Schiefelbein, 1999; Walker et al., 1999). When these genes are mutated, ectopic root hairs are formed from N cells. The bHLH transcription factors GLABRA3 (GL3) and ENHANCER OF GLABRA3 (EGL3) also function to specify hairless cells in a redundant manner, and ectopic root hairs form from N cells in *gl3 egl3* double mutants (Payne et al., 2000; Bernhardt et al., 2003; Zhang

[1] Current address: Kazusa DNA Research Institute, Kisarazu, Chiba 292-0818, Japan.
[2] Current address: Nano-Medicine Merger Education Unit, Institute for Frontier Medical Sciences, Kyoto University, Sakyo-ku, Kyoto 606-8507, Japan.
[3] Current address: Boyce Thompson Institute for Plant Research, Tower Road, Ithaca, NY 14853.
[4] Current address: 694 Futago, Aki, Higashikunisaki, Oita 873-0356, Japan.
[5] Current address: Forestry Research Institute, Oji Paper Company, Kameyama, Mie 519-0212, Japan.
[6] Current address: National Institute for Basic Biology, Myodaiji, Okazaki, Aichi 444-8585, Japan.
[7] Address correspondence to twada@psc.riken.jp.
The author responsible for distribution of materials integral to the findings presented in this article in accordance with the policy described in the Instructions for Authors (www.plantcell.org) is: Takuji Wada (twada@psc.riken.jp).
[W] Online version contains Web-only data.
www.plantcell.org/cgi/doi/10.1105/tpc.107.052274

et al., 2003). *GL2* expression is promoted by *WER*, *TTG1*, *GL3*, and *EGL3* in N cells (Hung et al., 1998; Lee and Schiefelbein, 1999; Bernhardt et al., 2003). GL3 and EGL3 interact with WER and TTG1, and the WER protein binds to two MYB binding sites in the *GL2* promoter, suggesting that a transcriptional complex consisting of WER, GL3/EGL3, and TTG1 directly regulates *GL2* transcription (Payne et al., 2000; Bernhardt et al., 2003; Zhang et al., 2003; Koshino-Kimura et al., 2005).

In contrast with the factors described above, *CAPRICE* (*CPC*), which encodes an R3 MYB protein, is required to specify hair cells, resulting in fewer hair cells in *cpc* mutants (Wada et al., 1997). *CPC* transcription in N cells is regulated by the WER-GL3/EGL3-TTG1 transcriptional complex as well as *GL2*, but the CPC protein moves from N cells to H cells (Lee and Schiefelbein, 2002; Wada et al., 2002; Bernhardt et al., 2003). *CPC* negatively regulates *GL2* and itself in a feedback repression loop in H cells (Lee and Schiefelbein, 2002; Wada et al., 2002). Because CPC interacts with GL3 and EGL3, it likely competes with WER for binding to bHLH and inhibits the formation of the WER-GL3/EGL3-TTG1 transcriptional complex in H cells (Zhang et al., 2003).

The same or homologous genes also function in trichome initiation. GLABROUS1 (GL1), which is functionally equivalent to WER, is thought to form a transcriptional complex with GL3/EGL3 and TTG1 to promote *GL2* expression in trichomes (Szymanski et al., 1998; Payne et al., 2000; Lee and Schiefelbein, 2001; Zhang et al., 2003). Mutations in *GL1*, *GL3*, *EGL3*, *TTG1*, and *GL2* result in a reduction in trichome number and less-branched trichomes, except for mutants with the *gl3-sst* allele (Koornneef et al., 1982; Esch et al., 2003; Zhang et al., 2003). *CPC* and its homolog, *TRIPTYCHON* (*TRY*), are transcribed in trichomes and affect trichome distribution (Schellmann et al., 2002). The number of trichomes is increased in *cpc* mutants, and trichomes are often clustered in *try* mutants (Schellmann et al., 2002). These mutant phenotypes suggest that *CPC* and *TRY* suppress trichome initiation by lateral inhibition. It has been proposed that CPC and TRY translated in trichomes move to neighbor epidermal cells, where they prevent GL1–GL3/EGL3 interaction by competition with GL1 for GL3/EGL3 binding sites (Esch et al., 2003).

Metabolic processes such as flavonoid biosynthesis and seed coat mucilage deposition are also regulated by transcriptional complexes consisting of an R2R3 MYB transcription factor, a bHLH transcription factor, and TTG1. Anthocyanins accumulate in vegetative tissues and are regulated by two *R2R3 MYB* genes, *PRODUCTION OF ANTHOCYANIN PIGMENT1* (*PAP1*) and *PAP2*, and three *bHLH* genes, *GL3*, *EGL3*, and *TRANSPARENT TESTA8* (*TT8*) (Borevitz et al., 2000; Zhang et al., 2003). Proanthocyanidin accumulation in seed coats is regulated by an *R2R3 MYB* gene, *TRANSPARENT TESTA2* (*TT2*), and a *bHLH* gene, *TT8* (Nesi et al., 2000, 2001). Seed coat mucilage production is regulated by an *R2R3 MYB* gene, *MYB61*, and two *bHLH* genes, *EGL3* and *TT8*, although the MYB61–EGL3/TT8 interaction has not been experimentally confirmed (Penfield et al., 2001; Zhang et al., 2003). *TTG1* is involved in all of these processes (Koornneef, 1981).

In addition to these regulatory genes, *TRANSPARENT TESTA GLABRA2* (*TTG2*) also regulates epidermal cell differentiation and metabolite accumulation. The *ttg2* mutant has apparent phenotypic defects in trichome development, proanthocyanidin and mucilage accumulation in seed coats, and integument cell elongation but not in differentiation into root hair or hairless cells (Johnson et al., 2002; Garcia et al., 2005). *TTG2* encodes a WRKY transcription factor and is expressed in leaf blades, trichomes, developing seeds, and the N cells of roots (Johnson et al., 2002). *TTG2* expression was previously shown to be very weak or absent in the leaf blades and seed coats of *ttg1-1* mutants, suggesting that *TTG2* is downstream of *TTG1* in the regulatory cascade (Johnson et al., 2002). Because TTG1 is thought to form a complex with R2R3 MYB and bHLH transcription factors, *R2R3 MYB* and *bHLH* genes are also likely to act upstream of *TTG2*, although this has not been demonstrated experimentally. *TTG2* also shares some activity with *GL2* in trichome development, because *gl2 ttg2* double mutants had more severe defects than either of the single mutants (Johnson et al., 2002). However, compared with the well-analyzed genetic relationships among *R2R3 MYB*, *R3 MYB*, *bHLH*, *WD40* (*TTG1*), and *HD-ZIP* (*GL2*) genes, the relationship between *TTG2* and these regulatory genes is not yet clear. To understand the relationship between *TTG2* and these other regulatory genes, we analyzed the transcriptional regulation of *TTG2* and its effects on the other regulators using a *TTG2* chimeric repressor in transgenic plants. Our results show that R2R3 MYB transcription factors directly promote *TTG2* expression and that *TTG2* could have a role in regulating *GL2* expression.

RESULTS

Determination of the *TTG2* Coding Region

TTG2 is predicted to encode a 428–amino acid protein, although a cDNA clone covering the whole predicted coding region has not yet been reported (Johnson et al., 2002). To confirm this prediction, we performed rapid amplification of cDNA ends (RACE)–PCR. The longest available *TTG2* cDNA was 1816 nucleotides long, with an open reading frame (ORF) of 428 amino acids, as predicted previously (Figure 1A) (Johnson et al., 2002). A comparison of the cDNA clone with the genomic sequence indicated that a 253-bp sequence upstream of the first ATG is divided into 245 bp and 8 bp by a 184-bp intron (Figure 1A). Sequencing of several RACE-PCR products revealed that alternative splicing occurs at the third intron (Figure 1A). In one of eight 5′ RACE-PCR products and one of four 3′ RACE-PCR products, the acceptor site of the third intron was 6 bp downstream of the previously reported site, resulting in a TTG2 protein that is shortened by two amino acids. It is unknown whether both versions of TTG2 protein are active or whether they both exist in the cell, and if they are, which version is more active.

To determine whether the first ATG is the actual translation start site, constructs were made using either an intact genomic *TTG2* clone containing the sequence from 1977 bp upstream of the first ATG to 426 bp downstream of the stop codon (FC) or construct FC with a CTC in place of the first ATG (FxC). In the FxC construct, the next ATG was at codon 81 (Figure 1A). These constructs were introduced into the *ttg2-1* mutant, which is likely to be a null mutant because of the transposition of *Tag1* into the

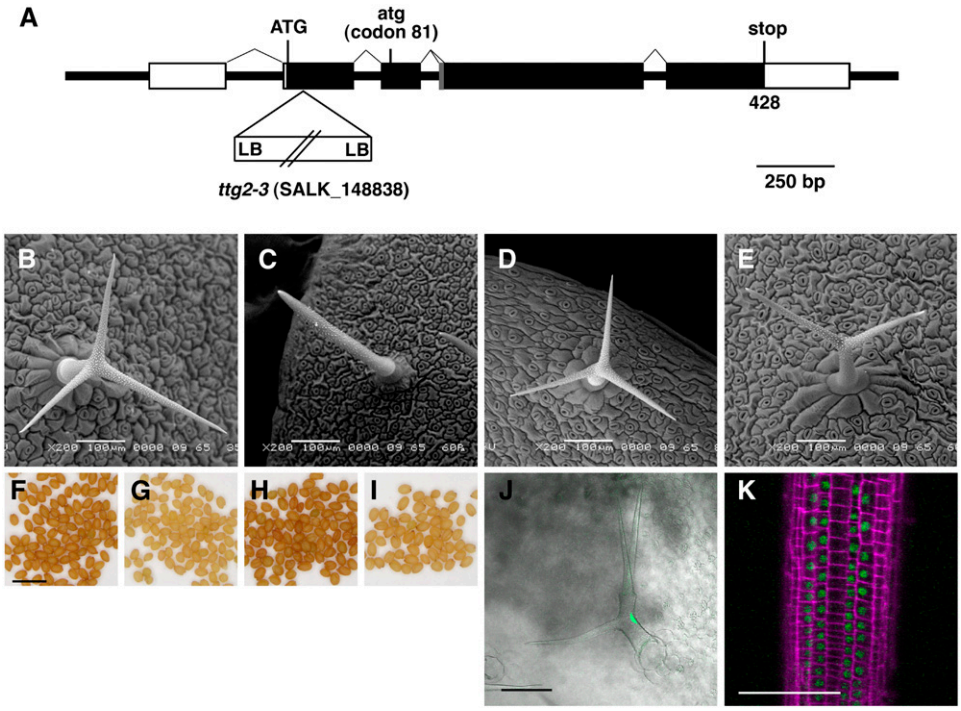

Figure 1. Determination of *TTG2* Gene Structure and Localization of the TTG2 Protein.

(A) Schematic of the *TTG2* gene. Boxes represent exons; closed boxes represent coding regions, and the gray bar in the fourth exon is absent from cDNA with alternative splicing. The ATG at codon 81 is indicated by lowercase letters. T-DNA is inserted into the second exon in the *ttg2-3* mutant. LB, left border.

(B) to **(E)** Scanning electron micrographs of trichomes of the wild type (Landsberg *erecta* [*Ler*]) **(B)**, *ttg2-1* **(C)**, *ttg2-1* transformed with the FC construct **(D)**, and *ttg2-1* transformed with the FxC construct **(E)**.

(F) to **(I)** Seed coat colors of the wild type (*Ler*) **(F)**, *ttg2-1* **(G)**, *ttg2-1* transformed with the FC construct **(H)**, and *ttg2-1* transformed with the FxC construct **(I)**.

(J) and **(K)** Confocal images of trichome and root expressing TTG2:2xGFP. Cell wall stained with propidium iodide is colored in magenta in **(K)**.

Bars in **(B)** to **(E)** and **(J)** and **(K)** = 100 μm, and bar in **(F)** (for **[F]** to **[I]**) = 1 mm.

third exon (Johnson et al., 2002). In the wild type, most leaf trichomes are three-branched and the seed color is brown (Figures 1B and 1F). *ttg2-1* mutants have mostly unbranched trichomes and pale brown seeds (Figures 1C and 1G). Construct FC restored wild-type trichome development and seed coat color (Figures 1D and 1H). The *ttg2-1* line transformed with construct FxC had trichomes that were two-branched, and its seed coat color was intermediate between the wild type and *ttg2-1* (Figures 1E and 1I). This result suggests that translation from the first ATG is needed for full function of the TTG2 protein. The TTG2 protein is a WRKY transcription factor that has a putative nuclear localization signal. We made the *ProTTG2:TTG2:2xGFP* construct to show that the TTG2:2xGFP fusion protein accumulates in trichomes and root N cell nuclei (Figures 1J and 1K). Also, this construct complemented the *ttg2* mutant, suggesting that the TTG2:2xGFP fusion protein is functionally equivalent to TTG2.

Double Mutant Phenotype

Mutations in *TTG2* cause defects in trichome development but not in roots. Several transcriptional regulators are known to be involved in the early stages of trichome development in *Arabidopsis*. To make it clear where in the regulatory network *TTG2* falls, *gl3-1 ttg2-1*, *gl3-2 ttg2-1*, and *try-82 ttg2-1* double mutants were generated. The *ttg1-1 ttg2-1*, *gl1-1 ttg2-1*, and *gl2-1 ttg2-1* double mutants have already been analyzed (Johnson et al., 2002). Phenotypes of *ttg1-1 ttg2-1* and *gl1-1 ttg2-1* are the same as in the single mutants *ttg1-1* and *gl1-1*, respectively. Trichome development in *gl2-1 ttg2-1* is more defective than in either single mutant. These results indicate that *TTG2* functions downstream of *TTG1* and *GL1* in the regulatory cascade and shares functions with *GL2* in trichome development.

Both *gl3* mutant alleles (*gl3-1* and *gl3-2*) produce reduced trichome numbers, and most trichomes have two branches (Figures 2A and 2E). In the *gl3 ttg2* double mutant, a few small pointed outgrowths were observed, which may be rudimentary trichomes (Figures 2B and 2E). This result suggests that *TTG2* and *GL3* cooperatively regulate trichome initiation and outgrowth.

Trichomes on *try-82* mutants are often clustered, and many trichomes have more than three branches (Figures 2C and 2E). Most of the trichomes on the *try-82 ttg2-1* double mutant were unbranched and similar to those of *ttg2-1* (cf. Figures 1C and 2D).

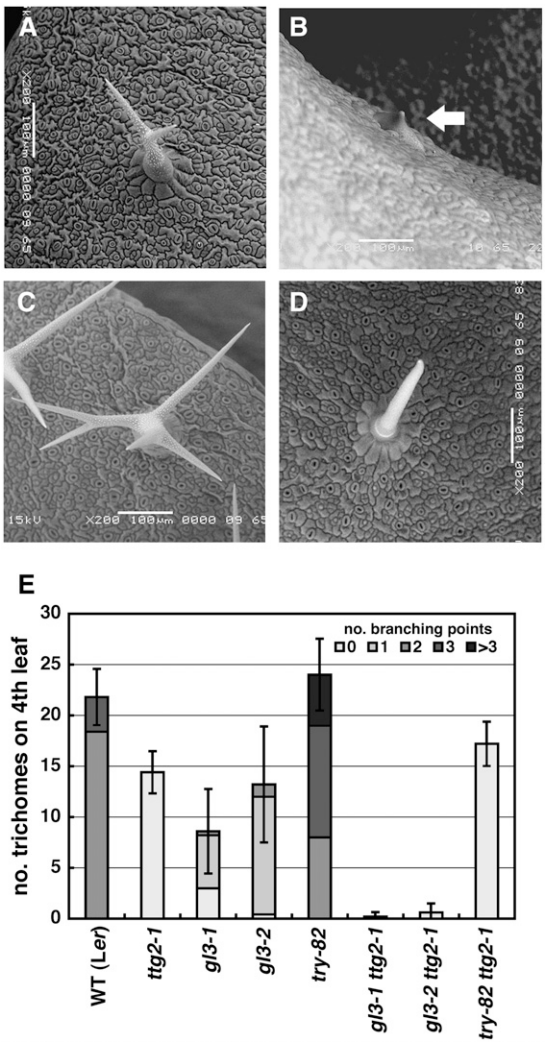

Figure 2. Trichome Phenotypes of Double Mutants.

(A) to **(D)** Scanning electron micrographs of trichomes of *gl3-2* **(A)**, *gl3-2 ttg2-1* **(B)**, *try-82* **(C)**, and *try-82 ttg2-1* **(D)**. The arrow indicates a trichome-like structure in **(B)**. Bars = 100 μm.

(E) Number of trichomes on fourth leaves of each genotype. Means ± SD of five plants of each genotype are shown. Trichomes are classified depending on the number of branch points. Plants were grown on soil for 21 d under continuous light.

The number of trichomes was also similar to that in *ttg2-1* (Figure 2E). Although some trichomes of *ttg2* were also clustered, there was no obvious increase of trichome clustering in *try-82 ttg2-1*. These results suggest that *ttg2* is epistatic to *try* in trichome development.

TTG2 Expression in Trichome and Root Hair Mutants

TTG2 is expressed in young leaves, petioles, trichomes, N cells of developing roots, and seed coats (Figures 3A and 3D) (Johnson et al., 2002). Previous analysis of *TTG2* expression in *ttg1-1*, *gl1-1*, *gl2-1*, and *ttg2-1* mutant lines indicates that *TTG1* is necessary for *TTG2* expression in young leaves and in the endothelium of seed coats (Johnson et al., 2002). To find other genes that regulate *TTG2* expression, we examined *TTG2* expression in several trichome and root hair mutants. We used a *ProTTG2:GUS* line, containing the pXH2.2 construct, or *ProTTG2(2.0):GFPGUS*, which is similar to pXH2.2 but with a green fluorescent protein:β-glucuronidase (GFP:GUS) fusion protein reporter rather than GUS (Johnson et al., 2002).

There was no GUS staining in the roots of *wer-1* and the *gl3-7454 egl3-5712* double mutant (Figures 3B and 3J). Conversely, ectopic GUS staining was detected in some H cells of the *cpc-2* single mutant and in all H cells of the *cpc-2 try-29760* double mutant (Figures 3E and 3G). These results suggest that *WER*, *GL3*, and *EGL3* positively regulate *TTG2* expression in N cells of roots and that *CPC* and *TRY* repress *TTG2* expression in H cells. Repression of *TTG2* expression by *CPC* was confirmed with *Pro35S:CPC* transgenic plants, in which GUS staining in roots, young leaves, leaf blades, and petioles was reduced (Figure 3C). GUS staining of leaf blades and petioles was also reduced in *egl3-5712*, and the reduction was enhanced by the addition of the *gl3-7454* mutation (Figures 3I and 3J). These results also suggest that *GL3* and *EGL3* positively and cooperatively regulate *TTG2* expression in leaf blades. Lastly, GUS staining was observed in the trichomes of all mutants if they formed trichomes.

Analysis of the *TTG2* Promoter

Previous analysis of the *TTG2* promoter suggested that a 5′ regulatory region extending from −703 to −300 regulates expression in trichomes, seed coats, and other tissues and that a 5′ region from −1000 to −703 regulates expression in roots (Johnson et al., 2002). *TTG2* expression was examined in a series of transgenic plants with deletions or base substitutions in the 5′ regulatory region of the *TTG2* gene to define elements of the upstream region that are critical for regulation.

The construct *ProTTG2(0.7):GFPGUS*, which has the same 5′ regulatory and translated regions as pEH0.7, was used to confirm previous results (Johnson et al., 2002). Strong GUS staining was detected in trichomes, petioles, and young leaves of *ProTTG2(0.7):GFPGUS* plants. Patchy staining was also detected in leaf blades (Figure 4A). These staining patterns were quite similar to those seen in *ProTTG2(2.0):GFPGUS*. Although it was reported that the pEH0.7 construct generated only very weak staining in root N cells even after 24 h of staining, 1 h was sufficient to give strong staining in the *ProTTG2(0.7):GFPGUS* construct (Figures 4A and 5) (Johnson et al., 2002). GUS staining was also detected in the trichomes, petioles, leaf primordia, and root N cells of *ProTTG2(0.6):GFPGUS* (Figure 5). GUS staining in *ProTTG2(0.5):GFPGUS* was not detected in trichomes themselves, but at their basal regions, and was restricted to the root cap (Figures 4C and 5). In *ProTTG2(0.7Δ4):GFPGUS*, GUS staining in leaves was similar to that of *ProTTG2(0.5):GFPGUS*, and it was weak and patchy in N cells and the root cap (Figures 4E and 5). These results strongly suggest that at least one *cis*-acting element responsible for *TTG2* expression in trichomes and roots resides in a region between −609 and −495. We searched for *cis* regulatory elements in the PLACE (for Plant *cis*-Acting Regulatory DNA Elements) database and found four

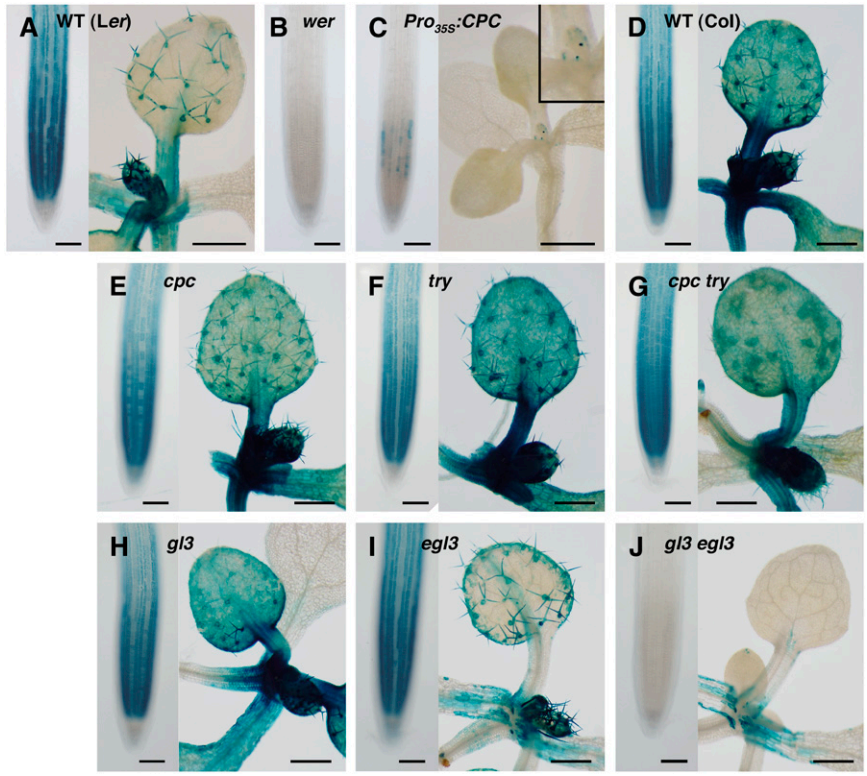

Figure 3. *TTG2* Expression in Mutants.

TTG2 expression in mutants was examined in *ProTTG2:GUS* lines containing construct pXH2.2 [**(A)** to **(C)**] and *ProTTG2(2.0):GFPGUS* [**(D)** to **(J)**].
(A) GUS staining pattern of the pXH2.2 line in the wild type (L*er*). Staining was detected in root N cells (left) and in young leaves, petioles, and trichomes (right).
(B) No GUS staining was detected in *wer-1* roots.
(C) In the *Pro35S:CPC* line, some patchy GUS staining was detected in roots (left). GUS staining of young leaves was very weak, and a few GUS-stained trichomes were observed (inset).
(D) GUS staining pattern of the *ProTTG2(2.0):GFPGUS* line in the wild type (Col-0). Leaf blades stained more intensely than those of the pXH2.2 line. Other tissues stained similarly to those of the pXH2.2 line.
(E) In *cpc-2*, ectopic GUS staining was detected in some root H cells. Staining in aerial parts was similar to that in the wild type.
(F) In *try-29760*, staining was similar to that in the wild-type.
(G) In the *cpc-2 try-29760* double mutant, GUS staining was detected in all epidermal root cells. GUS staining in young leaves and trichomes was similar to that in the wild type, but expression in trichomes did not last as long as in the wild type.
(H) In *gl3-7454*, GUS staining was similar to that in the wild type.
(I) In *egl3-5712*, GUS staining of roots was the same as in the wild type. The staining of leaf blades and petioles was reduced, but trichomes were fully stained.
(J) In the *gl3-7454 egl3-5712* double mutant, GUS staining was detected in leaf and cotyledon petioles but not in roots.
Bars in root images = 100 μm, and bars in seedling images = 0.5 mm.

putative MYB binding sites within this region (Higo et al., 1999). Because two putative MYB binding sites (−568 to −563 and −567 to −560) partially overlap, the −568 to −560 sequence was designated M1 (AAACCAAAC) (Figure 5). Other putative binding sites located from −531 to −525 and −514 to −508 were designated M2 and M3, respectively (Figure 5). The sequences of M2 and M3 are identical (AACTAAC).

To determine which of the sites are important for *TTG2* expression, reporter gene expression under the control of the 5′ regulatory region from −703 to −1 with base substitutions was measured. M1 was mutated from AAACCAAAC to AAtttAAAC, and M2 and M3 were changed from AACTAAC to gcagAAC. GUS staining in *ProTTG2(0.7m1):GFPGUS*, *ProTTG2(0.7m2):GFPGUS*, *ProTTG2(0.7m3):GFPGUS*, *ProTTG2(0.7m1m2):GFPGUS*, and *ProTTG2(0.7m1m3):GFPGUS* was similar to that in *ProTTG2(0.7):GFPGUS* (Figure 5). In *ProTTG2(0.7m2m3):GFPGUS* and *ProTTG2(0.7m1m2m3):GFPGUS*, root staining was similar to that in *ProTTG2(0.7Δ4):GFPGUS* (Figures 4G and 5). These results suggest that either M2 or M3 would be necessary to express *TTG2* in the N cells of roots. No difference

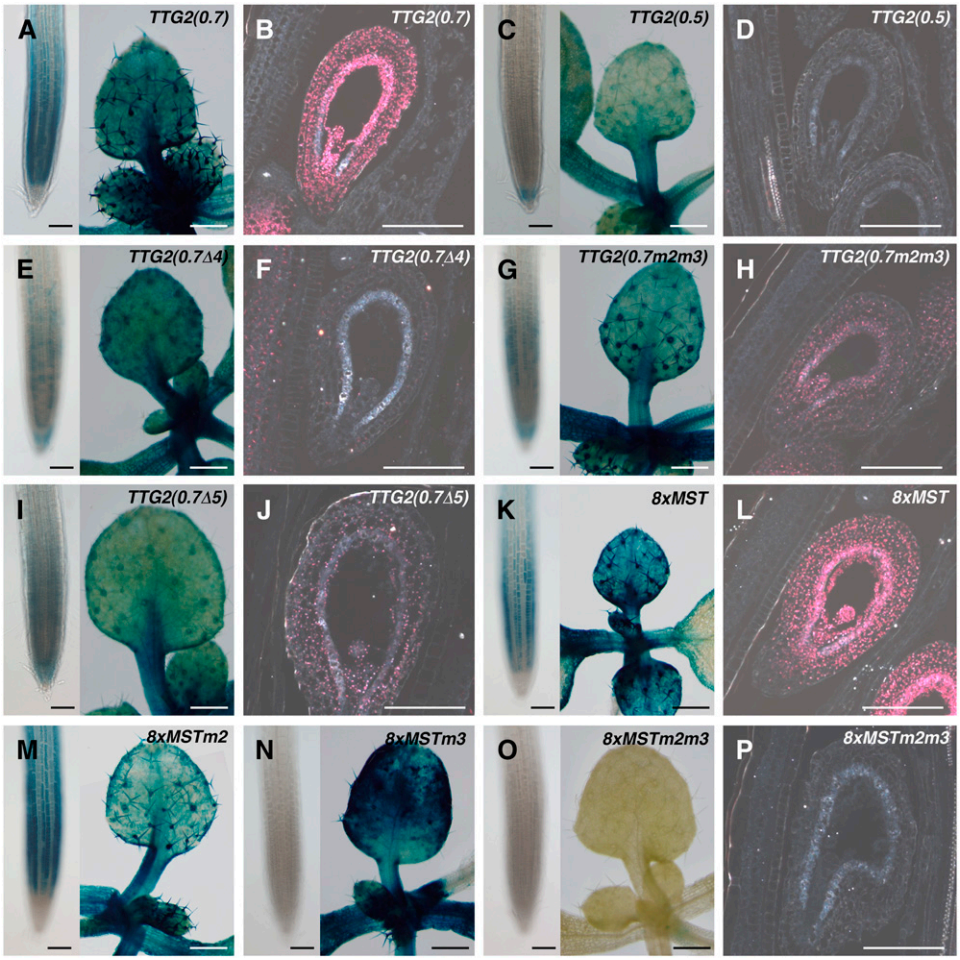

Figure 4. GUS Expression with Modified *TTG2* Promoters.

Seed samples were sectioned and observed under dark-field conditions, in which GUS staining appears pink (**[B]**, **[D]**, **[F]**, **[H]**, **[J]**, **[L]**, and **[P]**).
(A), **(C)**, **(E)**, **(G)**, **(I)**, **(K)**, **(M)**, **(N)**, and **(O)** GUS staining of root tips (left) and aerial parts of seedlings (right) of the *ProTTG2(0.7):GFPGUS*, *ProTTG2(0.5):GFPGUS*, *ProTTG2(0.7Δ4):GFPGUS*, *ProTTG2(0.7m2m3):GFPGUS*, *ProTTG2(0.7Δ5):GFPGUS*, *Pro8xMST:GFPGUS*, *Pro8xMSTm2:GFPGUS*, *Pro8xMSTm3:GFPGUS*, and *Pro8xMSTm2m3:GFPGUS* lines, respectively.
(B), **(D)**, **(F)**, **(H)**, **(J)**, **(L)**, and **(P)** Longitudinal sections of GUS-stained young seeds of the *ProTTG2(0.7):GFPGUS*, *ProTTG2(0.5):GFPGUS*, *ProTTG2(0.7Δ4):GFPGUS*, *ProTTG2(0.7m2m3):GFPGUS*, *ProTTG2(0.7Δ5):GFPGUS*, *Pro8xMST:GFPGUS*, and *Pro8xMSTm2m3:GFPGUS* lines, respectively.
Bars in root and seed images = 100 μm, and bars in seedling images = 0.5 mm.

was observed between GUS staining in *ProTTG2(0.7m2m3):GFPGUS* and *ProTTG2(0.7m1m2m3):GFPGUS*, indicating that M1 is not necessary as a *cis* regulatory element. To confirm this conclusion, we made construct *ProTTG2(0.7Δ5):GFPGUS*, whose promoter lacks the intervening region from M2 to M3. The GUS staining pattern was similar to that of *ProTTG2(0.7Δ4):GFPGUS*, suggesting that either M2 or M3 is necessary for *TTG2* expression in the N cells of roots, but M1 is not (Figure 4I).

To examine whether M2 or M3 alone would be sufficient for *TTG2* expression, we made four reporter constructs. An 8-mer of the 53-bp fragment from −546 to −494, which includes both M2 and M3 (MST), was fused to the cauliflower mosaic virus 35S minimal promoter to drive the reporter gene (Figure 5). Mutated MSTs (MSTm2, MSTm3, and MSTm2m3) were prepared to make similar constructs (Figure 5). GUS staining in Columbia (Col-0) transformants was detected in *Pro8xMST:GFPGUS*, *Pro8xMSTm2:GFPGUS*, and *Pro8xMSTm3:GFPGUS* transgenic lines but not in *Pro8xMSTm2m3:GFPGUS* (Figures 4K and 4M to 4O). Staining in *Pro8xMST:GFPGUS* was observed in trichomes and leaf blades (Figure 4K). Some lines showed GUS staining in N cells, but others did not (Figure 4K). GUS staining in the trichomes and leaf blades of *Pro8xMSTm2:GFPGUS* was similar to that of *Pro8xMST:GFPGUS* (Figure 4M). However, GUS staining in the roots of *Pro8xMSTm2:GFPGUS* lines was stronger than that in *Pro8xMST:GFPGUS* (Figures 4K and 4M). In *Pro8xMSTm3:GFPGUS*, staining was also observed in trichomes and leaf blades, although leaf blade staining

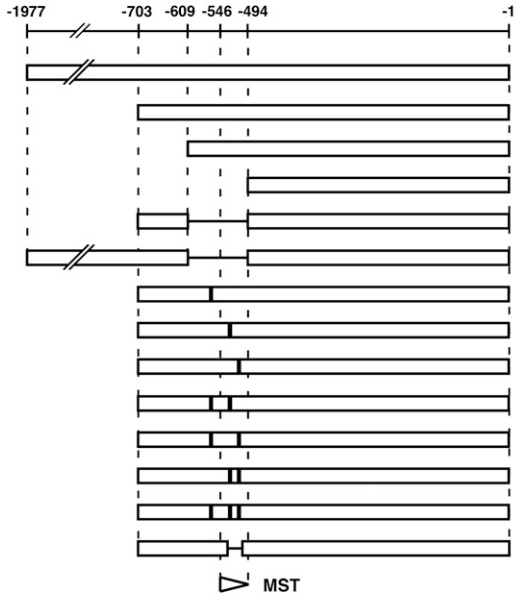

Promoter	GUS expression [a]			Complementation [b]
	trichome	root	seed	
TTG2(2.0)	++	++	n.a.	+
TTG2(0.7)	++	++	++	n.a.
TTG2(0.6)	++	++	n.a.	n.a.
TTG2(0.5)	–	–	–	n.a.
TTG2(0.7Δ4)	–	+ –	+ –	–
TTG2(2.0Δ4)	n.a.	n.a.	n.a.	+
TTG2(0.7m1)	++	++	n.a.	n.a.
TTG2(0.7m2)	++	++	n.a.	n.a.
TTG2(0.7m3)	++	++	n.a.	n.a.
TTG2(0.7m1m2)	++	++	n.a.	n.a.
TTG2(0.7m1m3)	++	++	n.a.	n.a.
TTG2(0.7m2m3)	++	+ –	+	n.a.
TTG2(0.7m1m2m3)	++	+ –	+	n.a.
TTG2(0.7Δ5)	–	+ –	+	– [c]
8xMST	++	+	++	+
8xMSTm2	++	++	++	+
8xMSTm3	++	–	++	+
8xMSTm2m3	–	–	–	–

Figure 5. Summary of *TTG2* Promoter Analysis.

A series of deletions and base substitutions in the 5′ regulatory region of the *TTG2* gene and their functions are summarized. At least 10 independent transgenic plants for each construct were examined. White boxes and arrowheads indicate the 5′ regulatory region of *TTG2* for each construct. Black stripes indicate the positions of putative MYB binding sites at which base substitutions were introduced. Gray boxes indicate the cauliflower mosaic virus 35S minimal promoter. [a] Relative levels of GUS expression are denoted as follows: ++, strong; +, moderate; + −, patchy (root) or faint (seed); −, not detected; n.a., not analyzed. [b] Whether or not trichome branching is rescued was examined: +, rescued; −, not rescued; n.a., not analyzed. [c] Among 49 T1 transformants, one plant had wild-type trichomes and others had *ttg2*-like trichomes.

appeared to be stronger than that of *Pro8xMST:GFPGUS* or *Pro8xMSTm2:GFPGUS* (Figures 4K, 4M, and 4N). No staining was observed in roots of *Pro8xMSTm3:GFPGUS* (Figure 4N).

Strong GUS staining was also observed in young embryos and all of the seed coat cell layers of *ProTTG2(0.7):GFPGUS*, *Pro8xMST:GFPGUS*, *Pro8xMSTm2:GFPGUS*, and *Pro8xMSTm3:GFPGUS* (Figures 4B, 4L, and 5). In *ProTTG2(0.7m2m3):GFPGUS*, *ProTTG2(0.7m1m2m3):GFPGUS*, and *ProTTG2(0.7Δ5):GFPGUS* lines, GUS intensity was weaker, but the pattern was similar to that of *ProTTG2(0.7):GFPGUS* (Figures 4H, 4J, and 5). Very weak GUS expression was detected in *ProTTG2(0.7Δ4):GFPGUS* (Figures 4F and 5), and no staining was observed in the embryos or seed coats of *ProTTG2(0.5):GFPGUS* or *Pro8xMSTm2m3:GFPGUS* (Figures 4D, 4P, and 5). These results suggest not only that M2 and M3 are required but that other elements are also important for *TTG2* expression in young ovules and developing seed coats.

The trichome defect of the *ttg2* mutant was rescued when *TTG2* was driven by the *Pro8xMST*, *Pro8xMSTm2*, or *Pro8xMSTm3* promoter (Figure 5). On the other hand, *TTG2* driven by *Pro8xMSTm2m3*, *ProTTG2(0.7Δ4)*, or *ProTTG2(0.7Δ5)* did not rescue the defects (Figure 5). Interestingly, when *TTG2* was driven by *ProTTG2(2.0Δ4)*, in which the region from −609 to −495 was removed from the full-length promoter, trichome defects were also rescued (Figure 5). Because the sequence from −949 to −943 is identical to M2, this region may be a MYB binding site.

Analysis of transgenic lines using the MST fragment suggests that MYB transcription factors bind to MST. WER is one of the binding candidates, because there was no *TTG2* expression in the roots of *wer-1* mutants. GL1 is also a binding candidate, because it is an early regulator of trichome development and because it is functionally equivalent to WER (Lee and Schiefelbein, 2001). TT2 may also be a candidate, because both *TT2* and *TTG2* are involved in proanthocyanidin accumulation in seed coats (Nesi et al., 2001; Johnson et al., 2002).

WER and TT2 bound strongly to MST and MSTm3 and significantly to MSTm2 in the yeast one-hybrid system assay (Figure 6). GL1 also bound significantly to MST (β-galactosidase units of pGAD-GL1 and pGAD424 transformants were 7.0 ± 0.6 and 1.2 ± 0.5 [mean ± SD], respectively) and apparently bound to MSTm2 and MSTm3 (Figure 6). Because the background activity of β-galactosidase is high in yeast containing the pLacZi-8xMSTm2m3 construct, it is difficult to determine whether or not WER, GL1, and TT2 bound to MSTm2m3. These results

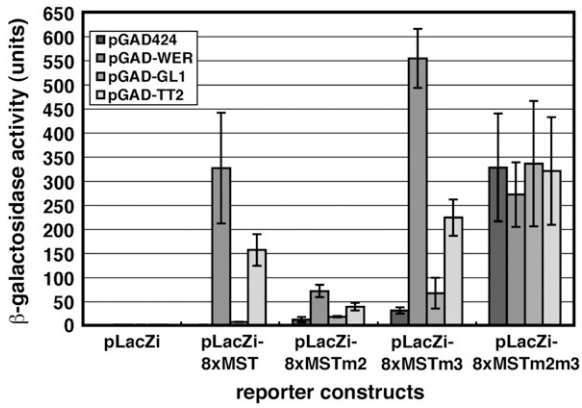

Figure 6. Yeast One-Hybrid Assays with R2R3 MYB Transcription Factors and the *TTG2* Promoter.

Yeast one-hybrid assays were used to examine the binding activities of WER, GL1, and TT2 to the MST, MSTm2, MSTm3, and MSTm2m3 fragments. pGAD424 is a negative control for effector plasmids, and pLacZi is a negative control for reporter plasmids. Data are presented as means ± SD from three independent experiments.

suggest that *TTG2* expression is directly regulated by *WER* in roots, by *GL1* in trichomes, and by *TT2* in developing seed coats. Although WER and GL1 are interchangeable in plants, their binding strengths to MST in yeast were very different (Lee and Schiefelbein, 2001). DNA binding activity and/or the stability of R2R3 MYB protein may differ, because R2R3 MYB proteins are solely expressed as chimeric proteins with the GAL4 activator domain in yeast one-hybrid assays, whereas R2R3 MYB proteins are thought to form a complex with bHLH proteins in planta (Payne et al., 2000; Bernhardt et al., 2003).

Expression of the Chimeric *TTG2* Repressor Resulted in *ttg1* Mutant Phenocopy

To determine whether *TTG2* regulates other transcription factors that regulate epidermal cell fate, *ProGL1:GUS*, *ProWER:GFP*, *ProCPC:GUS*, and *ProGL2:GUS* reporters were introduced into *ttg2-1* mutants. There were no apparent differences in GUS or GFP expression patterns between the wild type and *ttg2-1* mutants (Figure 7). It is thus unlikely that these genes function downstream of *TTG2* in the regulatory cascade.

Although *TTG2* is expressed in N cells, no phenotypic defects were observed in *ttg2* roots. This suggests that one or more other gene(s) compensates for the loss of *TTG2* function if *TTG2* plays a role in root development. To examine whether *TTG2* plays such a role in roots, we made transgenic plants expressing a chimeric protein in which TTG2 was fused with the modified EAR motif repression domain (SRDX), which should act as a dominant repressor (Hiratsu et al., 2003). No trichomes were formed on leaves, anthocyanins did not accumulate in hypocotyls, and ectopic root hairs were formed in the roots of 83 of 106 *ProTTG2:TTG2:SRDX* T1 transgenic lines (Figures 8I to 8K). Several glabrous lines were grown to examine their seed coats, which were pale yellow (Figure 8L). These phenotypes resembled those of the *ttg1* mutants (Figures 8M to 8P).

Real-time RT-PCR was used to compare the expression of seven genes known to influence root epidermal cell differentiation in the *ProTTG2:TTG2:SRDX* line with the wild type (Col-0) and *ttg2-3* (Figure 9A). The expression of six of the seven genes was similar between the wild type and *ttg2-3*, with *TTG2* as the exception. *GL2* expression was markedly reduced in *ProTTG2:TTG2:SRDX* lines compared with the wild type. *CPC* and endogenous *TTG2* expression were significantly reduced, whereas *GL3* expression was significantly higher, in at least one *ProTTG2:TTG2:SRDX* line. *WER* expression was somewhat lower, and *EGL3* expression was slightly higher, than in the wild type. *TTG1*

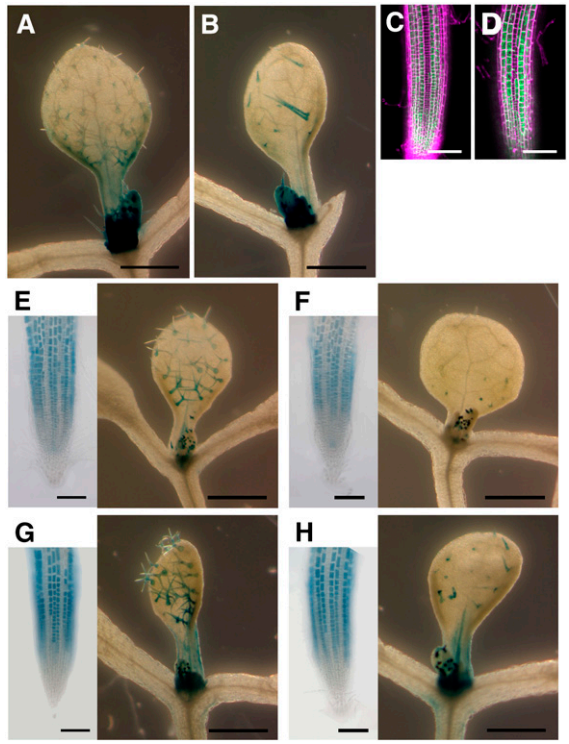

Figure 7. Gene Expression in the *ttg2* Mutant.

(A) *ProGL1:GUS* expression in the wild type. GUS staining was observed in young leaves and trichomes.
(B) *ProGL1:GUS* expression in the *ttg2-1* mutant. The GUS staining pattern was similar to that of the wild type **(A)**.
(C) *ProWER:GFP* expression in the wild type. GFP fluorescence was observed in N cells. Cell wall stained with propidium iodide is colored in magenta.
(D) *ProWER:GFP* expression in the *ttg2-1* mutant. The GFP fluorescence pattern was similar to that of the wild type **(C)**.
(E) *ProCPC:GUS* expression in the wild type. GUS staining was observed in N cells (left) and trichomes (right).
(F) *ProCPC:GUS* expression in the *ttg2-1* mutant. The GUS staining pattern was similar to that of the wild type **(E)**.
(G) *ProGL2:GUS* expression in the wild type. GUS staining was observed in N cells (left) and trichomes (right).
(H) *ProGL2:GUS* expression in the *ttg2-1* mutant. The GUS staining pattern was similar to that of the wild type **(G)**.
Bars in root images = 100 μm, and bars in seedling images = 0.5 mm.

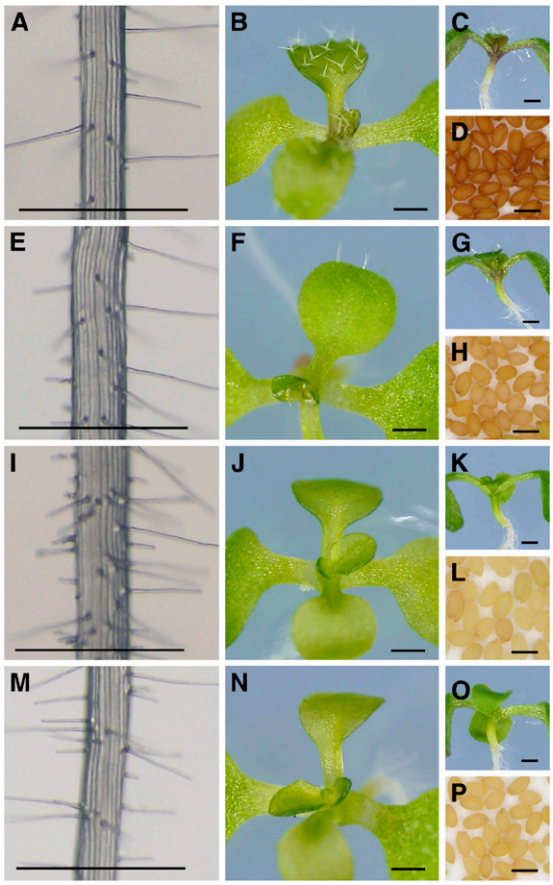

Figure 8. Phenotypes of *ProTTG2:TTG2:SRDX* Transgenic Plants.
Comparison of phenotypes of the *ProTTG2:TTG2:SRDX* transgenic plant (**[I]** to **[L]**) with that of the wild type (Col-0) (**[A]** to **[D]**), *ttg2-3* (**[E]** to **[H]**), and *ttg1-11* (**[M]** to **[P]**).
(A) Hairless cell files separate root hair cell files in wild-type roots.
(B) Wild-type leaves with three-branched trichomes.
(C) Anthocyanin is accumulated at the junction of the hypocotyl and cotyledons in wild-type seedlings.
(D) Seed coat color of the wild type is dark brown.
(E) Distribution of root hairs in *ttg2-3* is similar to that in the wild type **(A)**.
(F) The number of trichomes per leaf is reduced and most trichomes are unbranched in *ttg2-3*.
(G) Anthocyanin accumulation in *ttg2-3* is similar to that of the wild type **(C)**.
(H) Seed coat of *ttg2-3* is pale brown.
(I) Root hairs are formed from all cell files in *ProTTG2:TTG2:SRDX* transgenic plants.
(J) Glabrous leaves of *ProTTG2:TTG2:SRDX* transgenic plants.
(K) Anthocyanin is not accumulated in *ProTTG2:TTG2:SRDX* transgenic plants.
(L) Seed coat color of *ProTTG2:TTG2:SRDX* transgenic plants is much paler than that of *ttg2-3*.
(M) Root hair cell files are adjacent in *ttg1-11*.
(N) Glabrous leaves of *ttg1-11* are similar to those of *ProTTG2:TTG2:SRDX* transgenic plants.
(O) Anthocyanin is not accumulated in *ttg1-11* or in *ProTTG2:TTG2:SRDX* transgenic plants.
(P) Seed coat color of *ttg1-11* is similar to that of *ProTTG2:TTG2:SRDX* transgenic plants.
Bars = 0.5 mm.

expression was the same as in the wild type. Expression of four reporter constructs in *ProTTG2:TTG2:SRDX* lines was also examined. *ProGL2:GUS* was not detected in *ProTTG2:TTG2:SRDX* (Figure 9B), and expression of *ProTTG2:GFP:GUS* was reduced and nonspecific to N cells (Figure 9C). In the case of *ProCPC:GUS*, GUS staining was detected in the stele but not in the epidermis (Figure 9D). *ProWER:GFP* gave strong GFP fluorescence in N cells but weak fluorescence in H cells (Figure 9E). These results suggest that *TTG2* regulates the expression of *CPC*, *GL2*, and itself and that the repression of *GL2* by the TTG2:SRDX chimeric protein results in ectopic root hair formation.

DISCUSSION

The N-Terminal Region of TTG2 Is Important for Its Function

Although the *TTG2* gene had been shown to encode a WRKY transcription factor in a previous study, no full-length *TTG2* cDNA has been isolated (Johnson et al., 2002). In this study, RACE-PCR revealed that *TTG2* has an additional noncoding exon and that alternative splicing occurs at the third intron. An ORF of the longest *TTG2* cDNA corresponded to the predicted coding region (Johnson et al., 2002). The construct FxC, in which the first ATG of the ORF was changed to CTC, did not rescue the phenotypic defects of mutant line *ttg2-1* completely, providing evidence that, except for the possibility of a rare start codon, the first ATG of the ORF is the translation start site (Figures 1E and 1I).

The construct FxC only partially rescued trichome defects in *ttg2-1* mutants, as shown by the growth of two-branched trichomes (Figure 1E). Bifurcated trichomes were also observed in transformants of the *ttg2-1* line, which contained constructs in which a genomic *TTG2* fragment from the third to the fifth exons was driven by the cauliflower mosaic virus 35S promoter in the sense direction (data not shown). These results raise the possibilities that translation also occurs from the codon 81 ATG of the coding region and that a truncated protein that lacks the N-terminal region of TTG2 was produced from the FxC construct (Figure 1A). As the N terminus is rich in Ser and Thr, it is thought to be a transcription activation domain (Johnson et al., 2002). However, because the truncated TTG2 protein has other putative activation domains and motifs, such as WRKY domains and a nuclear localization signal, transcription activity may still be reduced (Johnson et al., 2002).

TTG2 Expression Is Regulated by *MYB*, *bHLH*, and *TTG1*

TTG2 plays a pleiotropic role in plant development and is expressed in several disparate organs. According to a previous study, *TTG2* expression in the *ttg1-1* mutant is patchy and less regular in roots than in the wild type, suggesting that *TTG1* positively regulates *TTG2* expression (Johnson et al., 2002). Our analyses demonstrate that *WER*, *GL3*, and *EGL3* positively regulate *TTG2* expression in N cells of wild-type roots (Figures 3B and 3J). The two identical MYB binding sites (M2 and M3) in the MST region of the *TTG2* promoter are clearly important for *TTG2* expression, and WER, a R2R3 MYB protein, binds to them

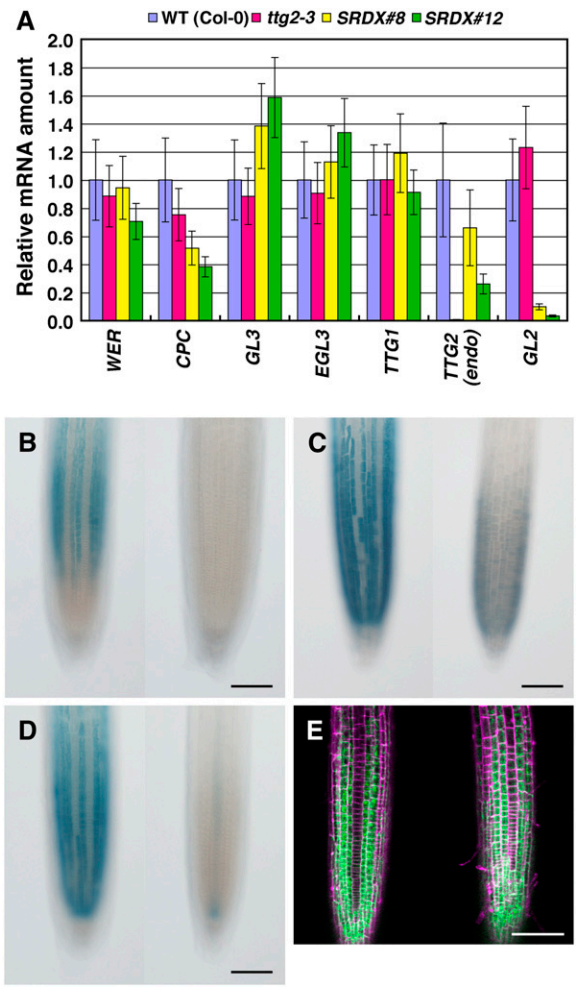

Figure 9. Gene Expression in Roots of *ProTTG2:TTG2:SRDX* Transgenic Plants.

Expression of genes involved in regulating the differentiation of root epidermis was analyzed by real-time RT-PCR and reporter constructs.
(A) Real-time RT-PCR analysis of *WER*, *CPC*, *GL3*, *EGL3*, *TTG1*, endogenous *TTG2* [*TTG2 (endo)*], and *GL2* expression in root tissue of the wild type (Col-0), *ttg2-3*, and two independent *ProTTG2:TTG2:SRDX* lines (*SRDX#8* and *SRDX#12*). Expression levels are given in relative units, with the wild-type level serving as 1 unit. The mean ± SD of four separate reactions (two replicates of each of two separate biological replicates) is indicated for each sample.
(B) Comparison of *ProGL2:GUS* expression in roots of the wild type (left) with that of *ProTTG2:TTG2:SRDX* transgenic plants (right).
(C) Comparison of *ProTTG2:GFPGUS* expression in roots of the wild type (left) with that of *ProTTG2:TTG2:SRDX* transgenic plants (right).
(D) Comparison of *ProCPC:GUS* expression in roots of the wild type (left) with that of *ProTTG2:TTG2:SRDX* transgenic plants (right).
(E) Comparison of *ProWER:GFP* expression in roots of the wild type (left) with that of *ProTTG2:TTG2:SRDX* transgenic plants (right). Cell wall stained with propidium iodide is colored in magenta.
Bars in **(B)** to **(E)** = 100 μm.

(Figures 4 to 6). Because the WER protein interacts with bHLH proteins, GL3, and EGL3, and GL3 and EGL3 interact with TTG1 in yeast, transcriptional complexes containing WER, GL3/EGL3, and TTG1 could directly promote *TTG2* expression in roots (Payne et al., 2000; Bernhardt et al., 2003; Zhang et al., 2003). In contrast with *WER*, *GL3*, and *EGL3*, *CPC* and *TRY* negatively regulate *TTG2* expression (Figures 3E and 3G). Both *CPC* and *TRY* encode R3 MYB proteins missing a domain that activates transcription (Wada et al., 1997; Schellmann et al., 2002). It has been proposed that R3 MYB proteins compete with R2R3 MYB transcription factors for binding to bHLH transcription factors to inhibit the formation of the regulatory complex (Esch et al., 2003, 2004). Accumulation of CPC and TRY proteins should inhibit the formation of WER-GL3/EGL3-TTG1 complexes and repress *TTG2* expression in H cells of wild-type roots and in all epidermal root cells of *Pro35S:CPC* plants.

TTG2 expression in trichomes, leaf blades, and seed coats is also likely to be directly promoted by R2R3 MYB-bHLH-TTG1 complexes. In trichomes, GL1-GL3/EGL3-TTG1 complexes should promote *TTG2* expression, as shown by the binding of GL1 to the MST region in yeast assays (Payne et al., 2000). In seed coats, TT2-TT8-TTG1 complexes should promote *TTG2* expression, because TT2 protein also binds the MST region in yeast assays (Baudry et al., 2004). *TTG2* expression in leaf blades was repressed in the *egl3*, *gl3 egl3*, and *ttg1* mutants (Johnson et al., 2002). In these mutants, anthocyanin accumulation is reduced in hypocotyls, cotyledons, and young leaves (Zhang et al., 2003). GL3 and EGL3 interact with the MYB domains of PAP1 and PAP2, which regulate anthocyanin production (Zhang et al., 2003). Because *TTG2* is upregulated in a *PAP1*-overexpressing line, *TTG2* transcription should be

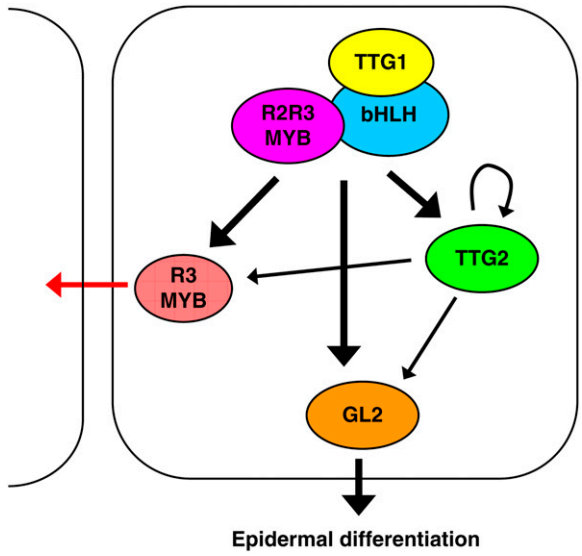

Figure 10. Proposed Model for *TTG2* in Epidermal Cell Differentiation.

Black arrows indicate positive regulation, and the thickness of the lines indicates degree of contribution. The red arrow indicates intercellular movement of the R3 MYB protein to inhibit interaction between R2R3 MYB and bHLH in adjacent cells.

positively regulated by a PAP1/PAP2-GL3/EGL3-TTG1 complex in leaf blades (Tohge et al., 2005).

Role of *TTG2* in Epidermal Differentiation

The CRES-T system, which was applied in the *TTG2:SRDX* experiment, uses a chimeric transcription factor with the EAR motif repression domain that functions as a dominant repressor (Hiratsu et al., 2003). *ProTTG2:TTG2:SRDX* lines had an enhanced *ttg2* phenotype (Figure 8), suggesting that TTG2 is a transcriptional activator and that the expression of TTG2's target genes would be repressed in *ProTTG2:TTG2:SRDX* lines.

In roots of the *ProTTG2:TTG2:SRDX* lines, *GL2*, *CPC*, and *TTG2* were significantly repressed, and downregulation of *GL2* resulted in ectopic root hair formation. Although they were directly downstream of *TTG1/WER/GL3/EGL3* in the regulatory cascade, expression of *TTG1*, *WER*, *GL3*, and *EGL3* were not significantly repressed (Figure 9), suggesting that *TTG2:SRDX* downregulates *GL2*, *CPC*, and *TTG2* without *TTG1*, *WER*, *GL3*, or *EGL3* (Koshino-Kimura et al., 2005; Ryu et al., 2005). This situation suggests that R2R3 MYB-bHLH-TTG1 complexes and TTG2 function together to regulate their common target genes (Figure 10). The severe trichome phenotype of *gl3 ttg2* double mutants supports this possibility (Figure 2B). However, the contribution of TTG2 could be smaller than that of R2R3 MYB-bHLH-TTG1 complexes, because *TTG2* expression itself depends on R2R3 MYB-bHLH-TTG1 complexes and there is no apparent difference in the expression of *GL2* and *CPC* between the wild type and *ttg2* mutants (Figures 7 and 9A). In addition, the extent of TTG2's contribution may be tissue-dependent. The effect of TTG2 in trichome development may thus be large enough that trichome defects can be observed in *ttg2* mutants, whereas it may be so small in roots that root hair defects are undetectable (Johnson et al., 2002). Downregulation of *GL2* by *TTG2:SRDX* may also cause the glabrous phenotype of *TTG2:SRDX* lines. However, strong *ProTTG2:TTG2:SRDX* lines are completely glabrous, whereas *gl2* mutants form immature trichomes. This inconsistency suggests that *TTG2:SRDX* suppresses *GL2* and other genes that have residual activity in trichome development of *gl2* mutants. *GL2* is one of the 16 class IV HD-ZIP (HD-ZIP IV) genes in *Arabidopsis*. Several members of this gene family are actually expressed in trichomes (Nakamura et al., 2006), and some of them may cooperatively regulate trichome development with *GL2*.

The anthocyanin-deficient and severe transparent testa phenotype of *ProTTG2:TTG2:SRDX* lines suggests that *TTG2* is involved in the regulation of both anthocyanin and proanthocyanidin accumulation. It has been reported that *ANTHOCYANINLESS2* (*ANL2*), a member of the HD-ZIP IV family, regulates anthocyanin accumulation in epidermal and subepidermal shoot cells (Kubo et al., 1999). However, *ANL2* was not one of the upregulated genes in *PAP1*-overexpressing plants in which *TTG2* was upregulated (Tohge et al., 2005). This suggests that *ANL2* is not downstream of *PAP1* in the regulation of anthocyanin biosynthesis. Another possibility is that *TTG2* regulates structural genes encoding enzymes such as dihydroflavonol reductase and leucoanthocyanidin dioxygenase, which are common in both anthocyanin and proanthocyanidin biosynthesis. A comparison of structural gene expression in the seeds and vegetative tissues of the wild type and *ttg2* may reveal some level of structure gene regulation by *TTG2*.

METHODS

Plant Materials and Growth Conditions

Arabidopsis thaliana ecotypes Col-0 or L*er* were used as the wild type. Except for transgenic plants generated for this study, plant materials are listed in Supplemental Table 1 online. Plants were grown in soil at 22°C under continuous light. Seeds were surface-sterilized and sown on 1.5% agar plates as described previously (Okada and Shimura, 1992) and grown out for observation of seedling phenotypes. In the experiment for anthocyanin accumulation, seeds were sown on 1.5% agar plates containing half-concentration Murashige and Skoog medium (Wako Pure Chemical) and 1.5% sucrose. Seeded plates were kept at 4°C for 4 d and then incubated at 22°C under continuous light.

RACE-PCR

Total RNA was extracted using an RNeasy plant mini kit (Qiagen). cDNA ends were amplified with the 5′ RACE system, version 2, and 3′ RACE system (Invitrogen) using total RNA from wild-type Col-0 seedlings. For 5′ RACE-PCR, primer TTG2-GSP0 was used for first-strand cDNA synthesis. Either TTG2-GSP1 or TTG2-GSP2 was used as the gene-specific primer for the first PCR amplification, and TTG2-GSP2 was used for the second amplification. The 5′ RACE-PCR product was digested with *Sal*I and *Cla*I and cloned into pBluescript II SK+. For 3′ RACE-PCR, either TTG2-B or TTG2-E was used as the gene-specific primer for the first PCR amplification, and TTG2-E was used for the second amplification. The 3′ RACE-PCR product was digested with *Bam*HI and *Spe*I and cloned into pBluescript II SK+. Ex Taq DNA polymerase (Takara) was used for cDNA amplification. Primer sequences are described in Supplemental Table 2 online.

Constructs and Plant Transformation

Plasmids for transgenic plants were constructed by standard techniques. Details are provided in the Supplemental Methods online. These constructs were subcloned into the pJHA212K binary vector (a gift from Ji Hoon Ahn) (Yoo et al., 2005) and introduced into *Agrobacterium tumefaciens* C58C1 or ASE. *Arabidopsis* plants (Col-0 wild type, *ttg2-1*, and *ttg2-3*) were transformed by the floral dipping method and screened on 0.8% agar plates containing half-concentration Murashige and Skoog medium and 50 mg/L kanamycin sulfate.

Real-Time RT-PCR

Total RNA was extracted from the roots of 5-d-old seedlings grown on 1.5% agar plates using the RNeasy plant mini kit (Qiagen). On-column DNase I digestion was done during RNA purification following the protocol in the RNeasy mini handbook. Extracted RNA was redigested with DNase I (amplification grade; Invitrogen) and then purified. First-strand cDNA was synthesized from 1 μg of total RNA in a 20-μL reaction mixture using a PrimeScript RT reagent kit (Takara). Real-time PCR was performed in a Chromo4 real-time PCR detection system (Bio-Rad) using SYBR Premix Ex Taq (Takara). PCR amplification had a 30-s denaturing step at 95°C, followed by 5 s at 95°C and 30 s at 60°C, with 40 cycles for *WER*, *CPC*, *GL3*, *EGL3*, *TTG1*, and *EF1*α and 50 cycles for endogenous *TTG2* and *GL2*. Relative mRNA levels were calculated by iQ5 software (Bio-Rad) and normalized to the concentration of *EF1*α mRNA.

The primers used were as follows: WER-qRTPCRf and WER-qRTPCRr for *WER*, CPC-qRTPCRf and CPC-R1 for *CPC*, GL3-qRTPCRf and GL3-qRTPCRr for *GL3*, EGL3-qRTPCRf and EGL3-qRTPCRr for *EGL3*, TTG1-qRTPCRf and TTG1-qRTPCRr for *TTG1*, TTG2en-qRTPCRf and TTG2-BB for endogenous *TTG2*, GL2-F and GL2-qRTPCRr for *GL2*, and RT-EF1α-F1 and RT-EF1α-R1 for *EF1α* (see Supplemental Table 2 online; Czechowski et al., 2004; Kwak and Schiefelbein, 2007).

GUS Staining and Observation

GUS staining of *Arabidopsis* transformants containing the *TTG2* reporter construct series was performed by fixing samples of the aerial parts of the plants in 90% ice-cooled acetone for 15 min, washing with staining buffer [50 mM Na-phosphate, pH 7.2, 3 mM $K_3Fe(CN)_6$, 3 mM $K_4Fe(CN)_6$, and 0.5% Triton X-100], and staining overnight at 37°C in staining buffer containing 2 mM X-Gluc (5-bromo-4-chloro-3-indolyl-β-glucronidase). Chlorophyll was removed with an increasing ethanol concentration series. Seedling samples were observed as whole mounts in 70% ethanol. Ovules were observed using dark-field optics by dehydrating silique samples before embedding in Technovit 7100 (Kulzer) for 8-μm sectioning. Root samples were stained directly for 1 h at 37°C in staining buffer containing 1 mM X-Gluc and observed as a whole mount in water. For the other constructs, $K_3Fe(CN)_6$ and $K_4Fe(CN)_6$ concentrations and/or incubation times were modified depending on the intensity of staining.

Scanning Electron Microscopy

Scanning electron microscopy samples were prepared and observed as described previously (Kurata et al., 2003).

Confocal Laser Scanning Microscopy

Roots were stained with 5 μg/mL propidium iodide for 30 s and mounted in water. Confocal images were obtained on Zeiss LSM-Pascal or LSM-510 Meta confocal laser scanning microscopes using 488- and 543-nm laser lines for excitation of GFP and propidium iodide, respectively. Images were processed with Adobe Photoshop version 6.0 (Adobe Systems).

Yeast One-Hybrid Assay

The construction of reporter and effector plasmids is described in the Supplemental Methods online. Reporter plasmids pLacZi-8xMST, pLacZi-8xMSTm2, pLacZi-8xMSTm3, pLacZi-8xMSTm2m3, and the intact pLacZi as a negative control were digested with *Apa*I and integrated into yeast strain YM4271 at the *URA3* locus. The resulting yeast strains were selected on SD medium lacking uracil. Three effector plasmids, pGAD-WER, pGAD-GL1, and pGAD-TT2, and the intact pGAD424 were transformed into yeast that had integrated each reporter plasmid. Following the Yeast Protocols Handbook (Clontech), a β-galactosidase assay was performed on each of three individual transformants using *o*-nitrophenyl β-D-galactopyranoside as substrate.

Accession Numbers

The GenBank/EMBL/DDBJ accession number for the *TTG2* cDNA investigated in this study is AB289607. The Arabidopsis Genome Initiative locus identifiers for the genes mentioned in this study are as follows: *TTG2* (At2g37260), *TTG1* (At5g24520), *GL2* (At1g79840), *GL3* (At5g41315), *EGL3* (At1g63650), *GL1* (At3g27920), *WER* (At5g14750), *TT2* (At5g35550), *CPC* (At2g46410), and *TRY* (At5g53200).

Supplemental Data

The following materials are available in the online version of this article.

Supplemental Table 1. Plant Materials Used in This Study.

Supplemental Table 2. Primers Used in Constructs and Assays.

Supplemental Methods. Construction of Plasmids.

ACKNOWLEDGMENTS

We thank Alan Lloyd, Martin Hulskamp, John Schiefelbein, David Marks, David Smyth, John C. Larkin, and the ABRC for providing *Arabidopsis* seeds and Ji Hoon Ahn, Yoshihiro Koshino-Kimura, and Alan Lloyd for providing plasmid materials. We also thank Kiminori Toyooka and Mayuko Sato for scanning electron microscopy analysis and Tetsuya Kurata and Rumi Tominaga for helpful discussions.

Received April 16, 2007; revised July 24, 2007; accepted August 14, 2007; published August 31, 2007.

REFERENCES

Baudry, A., Heim, M.A., Dubreucq, B., Caboche, M., Weisshaar, B., and Lepiniec, L. (2004). TT2, TT8, and TTG1 synergistically specify the expression of BANYULS and proanthocyanidin biosynthesis in *Arabidopsis thaliana*. Plant J. **39:** 366–380.

Bernhardt, C., Lee, M.M., Gonzalez, A., Zhang, F., Lloyd, A., and Schiefelbein, J. (2003). The bHLH genes *GLABRA3* (*GL3*) and *ENHANCER OF GLABRA3* (*EGL3*) specify epidermal cell fate in the Arabidopsis root. Development **130:** 6431–6439.

Borevitz, J.O., Xia, Y., Blount, J., Dixon, R.A., and Lamb, C. (2000). Activation tagging identifies a conserved MYB regulator of phenylpropanoid biosynthesis. Plant Cell **12:** 2383–2394.

Czechowski, T., Bari, R.P., Stitt, M., Scheible, W.R., and Udvardi, M.K. (2004). Real-time RT-PCR profiling of over 1400 Arabidopsis transcription factors: Unprecedented sensitivity reveals novel root- and shoot-specific genes. Plant J. **38:** 366–379.

Di Cristina, M., Sessa, G., Dolan, L., Linstead, P., Baima, S., Ruberti, I., and Morelli, G. (1996). The *Arabidopsis* Athb-10 (GLABRA2) is an HD-Zip protein required for regulation of root hair development. Plant J. **10:** 393–402.

Dolan, L., Duckett, C.M., Grierson, C., Linstead, P., Schneider, K., Lawson, E., Dean, C., Poethig, S., and Roberts, K. (1994). Clonal relationships and cell patterning in the root epidermis of *Arabidopsis*. Development **120:** 2465–2474.

Esch, J.J., Chen, M., Sanders, M., Hillestad, M., Ndkium, S., Idelkope, B., Neizer, J., and Marks, M.D. (2003). A contradictory *GLABRA3* allele helps define gene interactions controlling trichome development in *Arabidopsis*. Development **130:** 5885–5894.

Esch, J.J., Chen, M.A., Hillestad, M., and Marks, M.D. (2004). Comparison of TRY and the closely related At1g01380 gene in controlling Arabidopsis trichome patterning. Plant J. **40:** 860–869.

Galway, M.E., Masucci, J.D., Lloyd, A.M., Walbot, V., Davis, R.W., and Schiefelbein, J.W. (1994). The *TTG* gene is required to specify epidermal cell fate and cell patterning in the *Arabidopsis* root. Dev. Biol. **166:** 740–754.

Garcia, D., FitzGerald, J.N., and Berger, F. (2005). Maternal control of integument cell elongation and zygotic control of endosperm growth are coordinated to determine seed size in Arabidopsis. Plant Cell **17:** 52–60.

Higo, K., Ugawa, Y., Iwamoto, M., and Korenaga, T. (1999). Plant cis-acting regulatory DNA elements (PLACE) database: 1999. Nucleic Acids Res. **27:** 297–300.

Hiratsu, K., Matsui, K., Koyama, T., and Ohme-Takagi, M. (2003). Dominant repression of target genes by chimeric repressors that include the EAR motif, a repression domain, in *Arabidopsis*. Plant J. **34:** 733–739.

Hung, C.Y., Lin, Y., Zhang, M., Pollock, S., Marks, M.D., and Schiefelbein, J. (1998). A common position-dependent mechanism controls cell-type patterning and *GLABRA2* regulation in the root and hypocotyl epidermis of Arabidopsis. Plant Physiol. **117:** 73–84.

Johnson, C.S., Kolevski, B., and Smyth, D.R. (2002). *TRANSPARENT TESTA GLABRA2*, a trichome and seed coat development gene of Arabidopsis, encodes a WRKY transcription factor. Plant Cell **14:** 1359–1375.

Koornneef, M. (1981). The complex syndrome of *ttg* mutants. Arabidopsis Inf. Serv. **18:** 45–51.

Koornneef, M., Dellaert, L.W., and van der Veen, J.H. (1982). EMS- and radiation-induced mutation frequencies at individual loci in *Arabidopsis thaliana* (L.) Heynh. Mutat. Res. **93:** 109–123.

Koshino-Kimura, Y., Wada, T., Tachibana, T., Tsugeki, R., Ishiguro, S., and Okada, K. (2005). Regulation of *CAPRICE* transcription by MYB proteins for root epidermis differentiation in *Arabidopsis*. Plant Cell Physiol. **46:** 817–826.

Kubo, H., Peeters, A.J., Aarts, M.G., Pereira, A., and Koornneef, M. (1999). *ANTHOCYANINLESS2*, a homeobox gene affecting anthocyanin distribution and root development in Arabidopsis. Plant Cell **11:** 1217–1226.

Kurata, T., Kawabata-Awai, C., Sakuradani, E., Shimizu, S., Okada, K., and Wada, T. (2003). The *YORE-YORE* gene regulates multiple aspects of epidermal cell differentiation in *Arabidopsis*. Plant J. **36:** 55–66.

Kwak, S.H., and Schiefelbein, J. (2007). The role of the SCRAMBLED receptor-like kinase in patterning the Arabidopsis root epidermis. Dev. Biol. **302:** 118–131.

Lee, M.M., and Schiefelbein, J. (1999). WEREWOLF, a MYB-related protein in *Arabidopsis*, is a position-dependent regulator of epidermal cell patterning. Cell **99:** 473–483.

Lee, M.M., and Schiefelbein, J. (2001). Developmentally distinct MYB genes encode functionally equivalent proteins in *Arabidopsis*. Development **128:** 1539–1546.

Lee, M.M., and Schiefelbein, J. (2002). Cell pattern in the Arabidopsis root epidermis determined by lateral inhibition with feedback. Plant Cell **14:** 611–618.

Masucci, J.D., Rerie, W.G., Foreman, D.R., Zhang, M., Galway, M.E., Marks, M.D., and Schiefelbein, J.W. (1996). The homeobox gene *GLABRA2* is required for position-dependent cell differentiation in the root epidermis of *Arabidopsis thaliana*. Development **122:** 1253–1260.

Nakamura, M., Katsumata, H., Abe, M., Yabe, N., Komeda, Y., Yamamoto, K.T., and Takahashi, T. (2006). Characterization of the class IV homeodomain-leucine zipper gene family in Arabidopsis. Plant Physiol. **141:** 1363–1375.

Nesi, N., Debeaujon, I., Jond, C., Pelletier, G., Caboche, M., and Lepiniec, L. (2000). The *TT8* gene encodes a basic helix-loop-helix domain protein required for expression of *DFR* and *BAN* genes in Arabidopsis siliques. Plant Cell **12:** 1863–1878.

Nesi, N., Jond, C., Debeaujon, I., Caboche, M., and Lepiniec, L. (2001). The Arabidopsis *TT2* gene encodes an R2R3 MYB domain protein that acts as a key determinant for proanthocyanidin accumulation in developing seed. Plant Cell **13:** 2099–2114.

Okada, K., and Shimura, Y. (1992). Mutational analysis of root gravitropism and phototropism of *Arabidopsis thaliana* seedlings. Aust. J. Plant Physiol. **19:** 439–448.

Payne, C.T., Zhang, F., and Lloyd, A.M. (2000). GL3 encodes a bHLH protein that regulates trichome development in Arabidopsis through interaction with GL1 and TTG1. Genetics **156:** 1349–1362.

Penfield, S., Meissner, R.C., Shoue, D.A., Carpita, N.C., and Bevan, M.W. (2001). *MYB61* is required for mucilage deposition and extrusion in the Arabidopsis seed coat. Plant Cell **13:** 2777–2791.

Rerie, W.G., Feldmann, K.A., and Marks, M.D. (1994). The *GLABRA2* gene encodes a homeo domain protein required for normal trichome development in *Arabidopsis*. Genes Dev. **8:** 1388–1399.

Ryu, K.H., Kang, Y.H., Park, Y.H., Hwang, I., Schiefelbein, J., and Lee, M.M. (2005). The WEREWOLF MYB protein directly regulates *CAPRICE* transcription during cell fate specification in the *Arabidopsis* root epidermis. Development **132:** 4765–4775.

Schellmann, S., Schnittger, A., Kirik, V., Wada, T., Okada, K., Beermann, A., Thumfahrt, J., Jurgens, G., and Hulskamp, M. (2002). *TRIPTYCHON* and *CAPRICE* mediate lateral inhibition during trichome and root hair patterning in *Arabidopsis*. EMBO J. **21:** 5036–5046.

Szymanski, D.B., Jilk, R.A., Pollock, S.M., and Marks, M.D. (1998). Control of *GL2* expression in Arabidopsis leaves and trichomes. Development **125:** 1161–1171.

Tohge, T., et al. (2005). Functional genomics by integrated analysis of metabolome and transcriptome of Arabidopsis plants over-expressing an MYB transcription factor. Plant J. **42:** 218–235.

Wada, T., Kurata, T., Tominaga, R., Koshino-Kimura, Y., Tachibana, T., Goto, K., Marks, M.D., Shimura, Y., and Okada, K. (2002). Role of a positive regulator of root hair development, *CAPRICE*, in *Arabidopsis* root epidermal cell differentiation. Development **129:** 5409–5419.

Wada, T., Tachibana, T., Shimura, Y., and Okada, K. (1997). Epidermal cell differentiation in *Arabidopsis* determined by a *Myb* homolog, *CPC*. Science **277:** 1113–1116.

Walker, A.R., Davison, P.A., Bolognesi-Winfield, A.C., James, C.M., Srinivasan, N., Blundell, T.L., Esch, J.J., Marks, M.D., and Gray, J.C. (1999). The *TRANSPARENT TESTA GLABRA1* locus, which regulates trichome differentiation and anthocyanin biosynthesis in Arabidopsis, encodes a WD40 repeat protein. Plant Cell **11:** 1337–1350.

Yoo, S.Y., Bomblies, K., Yoo, S.K., Yang, J.W., Choi, M.S., Lee, J.S., Weigel, D., and Ahn, J.H. (2005). The 35S promoter used in a selectable marker gene of a plant transformation vector affects the expression of the transgene. Planta **221:** 523–530.

Zhang, F., Gonzalez, A., Zhao, M., Payne, C.T., and Lloyd, A. (2003). A network of redundant bHLH proteins functions in all TTG1-dependent pathways of *Arabidopsis*. Development **130:** 4859–4869.